

1 **Spatial heterogeneity in earthquake fault-like systems**

2

3

4

5 **J. Kazemian<sup>1</sup>, R. Dominguez<sup>2</sup>, K.F. Tiampo<sup>1</sup>, W. Klein<sup>3</sup>**

6

7 [1]{Department of Earth Sciences, Western University, London, Ontario N6A 5B7, Canada}

8 [2]{Department of Physics, Randolph-Macon College, Ashland, Virginia 23005, USA}

9 [3]{Department of Physics and Center for Computational Sciences, Boston University,  
10 Boston, Massachusetts 02215, USA}

11 Correspondence to: J. Kazemian (jkazemia@uwo.ca)

12

13

14

15

16

17

18

19

20

## 1 **Abstract**

2 The inhomogeneity of the materials with different physical properties in the Earth is  
3 responsible for a wide variety of spatial and temporal behaviors. In this work, we study an  
4 earthquake fault model based on Olami-Feder-Christensen (OFC) and Rundle-Jackson-Brown  
5 (RJB) cellular automata models with particular aspects of spatial heterogeneities and long-  
6 range stress interactions. In our model some localized stress accumulators are added into the  
7 system by converting a percentage of randomly selected sites into stronger sites which are  
8 called ‘asperity cells’. These asperity cells support much higher failure stresses than the  
9 surrounding regular lattice sites but eventually rupture when the applied stress reaches their  
10 threshold stress. We find that changing the spatial configuration of those stronger sites  
11 generally increases capability of the fault system to generate larger events, but that the total  
12 percentage of asperities is important as well. We also observe an increasing number of larger  
13 events associated with the total number of asperities in the lattice.

14

15 **Keywords:** Earthquake simulation; extreme events; GR scaling

16

## 17 **1 Introduction**

18 Despite the multitude of space-time patterns of activity observed in natural earthquake fault  
19 systems, the bulk of the research associated with these patterns has focused on a relatively  
20 small fraction of the events, those associated with either larger magnitudes or persistent,  
21 localized signals such as aftershock sequences [Kanamori, 1981; Ogata, 1983; Utsu et al.,  
22 1995]. One significant problem associated with studies of the earthquake fault network is that  
23 the underlying dynamics of the system are not observable [Herz and Hopfield, 1995; Rundle  
24 et al., 2000]. A second is that the nonlinear earthquake dynamics are strongly coupled across a

1 wide range of spatial and temporal scales [Kanamori, 1981; Main, 1996; Turcotte, 1997;  
2 Rundle et al., 1999; Scholz, 2002]. Finally, the relatively small number of extreme events  
3 occur very rarely, impacting our ability to evaluate the significance of the associated local and  
4 regional patterns in the instrumental and historic data [Schorlemmer and Gerstenberger, 2007;  
5 Vere-Jones, 1995, 2006; Zechar et al., 2010]. As a result, computational simulations are  
6 critical to enhancing our understanding of the dynamics of the earthquake system and the  
7 occurrence of its largest events [see, e.g., Rundle et al., 2003].

8 Although simple models cannot replicate the complete spectrum of earthquake  
9 phenomenology, these models can provide insights into the important patterns and features  
10 associated with the earthquake process and improve our understanding of the dynamics and  
11 underlying physics of earthquake fault networks. As a result, simple models of statistical  
12 fracture have been used to test some of the typical assumptions and parameters and their  
13 possible outcomes (Burridge and Knopoff, 1967; Otsuka, 1972; Rundle and Jackson, 1977;  
14 Rundle, 1988; Carlson and Langer, 1989; Nakanishi, 1990, Rundle and Brown, 1991; Olami  
15 et al., 1992; Alava et al. 2006). Most of these models assumed a spatially homogeneous  
16 earthquake fault, despite the fact that numerical and experimental models of rock fracture  
17 suggest that spatial inhomogeneities play an important role in the occurrence of large events  
18 and the associated spatial and temporal phenomenology [Dahmen et al., 1998; Turcotte et al.,  
19 2003; Tiampo et al., 2002, 2007; Lyakhovskiy and Ben-Zion, 2009]. One argument for this  
20 approach has been that earthquake faults have long-range stress transfer [Klein et al., 2007].  
21 For long-range stress transfer without inhomogeneities, or randomly distributed  
22 inhomogeneities, these models have been found to produce scaling similar to the Gutenberg-  
23 Richter (GR) scaling found in real earthquake systems [Gutenberg and Richter, 1956; Serino  
24 et al., 2011]. When the stress transfer range is longer than the length scales associated with  
25 the inhomogeneities in the system, the dynamics appear to be unaffected by the

1 inhomogeneities. However, recent work by Dominguez et al., [2013] shows that the ratio of  
2 the stress transfer range to the length scale of the inhomogeneities affects the GR scaling  
3 distribution and the ability of the system to produce large events.

4 The spatial arrangement of fault inhomogeneities is dependent on the geologic history of the  
5 fault. This history is typically quite complex and, as a result, the spatial distribution of the  
6 various inhomogeneities occurs on many length scales. Because spatial inhomogeneity plays  
7 an important role in the seismicity of an earthquake fault, here we extend the homogeneous  
8 OFC model with long-range stress transfer to inhomogeneous models, where particular  
9 parameters might vary from site to site.

10 There have been some earlier studies of the inhomogeneous OFC model (Janosi and Kertesz,  
11 1993; Torvund and Froyland, 1995; Ceva, 1995; Mousseau, 1996; Ramos et al. 2006; Bach et  
12 al., 2008; Jagla, 2010). Although, these models considered a number of different ways to  
13 impose inhomogeneity on the system, most only investigated systems with nearest neighbor  
14 or short-range stress transfer. For example, Janosi and Kertesz (1993) introduced spatial  
15 inhomogeneity into the lattice by imposing random site-dependent stress thresholds. Torvund  
16 and Froyland (1995) imposed inhomogeneity by changing the uniform distribution of  
17 threshold stresses to a Gaussian distribution. Ceva (1995) introduced defects associated with  
18 the stress transmission parameter. Ramos (2006) and Jagla (2010) considered varying levels  
19 of randomness in the stress threshold.

20 Serino et al. (2011) studied OFC models with long-range stress transfer in which random  
21 damage was incorporated into the lattice. Dominguez et al. (2013) studied the various spatial  
22 configurations of damage in a long-range stress transfer model with varying amounts of stress  
23 dissipation,  $\alpha$  ( $0 < \alpha \leq 1$ ) which describe the portion of stress dissipated from the failed sites.  
24 Both models represented damage by imposing live and dead sites in the lattice framework.

1 The live sites can hold an internal stress that is a function of time. Dead sites cannot hold any  
2 stress and therefore all the stress that is passed to them during an event is dissipated from the  
3 system. The amount of stress dissipated by damage sites at each location can be characterized  
4 by the percentage of dead sites in a given neighborhood,  $\phi_i$ . Serino et al. (2011) established a  
5 connection between the two types of dissipation, stress dissipation and damage dissipation,  
6 and Dominguez et al (2013) showed that they can be characterized together in one parameter,  
7  $\gamma_i$ , herein called site dissipation,  $\gamma_i = 1 - \phi_i(1 - \alpha_i)$ . Results showed that both stress dissipation  
8 and damage dissipation reduces the length of the scaling regime in their magnitude-frequency  
9 distributions and reduces the size of the largest events.

10 Dominguez et al. (2013) imposed various spatial patterns for the dead sites and compared the  
11 behavior with simpler systems with uniformly distributed stress dissipation. Figure 1 shows  
12 four different configurations of 25% dead sites for a lattice with linear size  $L = 256$ , stress  
13 dissipation  $\alpha = 0$ , and a stress transfer range of  $R = 16$ . These include one case with randomly  
14 distributed dead sites (random); a second with blocks of various sizes, where each block has  
15 varying values of randomly distributed dead sites (random cascading blocks); a third with  
16 completely dead blocks of various sizes (cascading dead blocks); and a fourth with dead  
17 blocks of a uniform size (dead blocks). The resulting numerical distribution of events of size  
18  $s$  for the various spatial distributions of dead sites shown is shown in Figure 1b. Here we see  
19 that the addition of spatial heterogeneity into the lattice *increases* the length of the scaling  
20 regime and the size of the largest events as the randomness of the spatial pattern decreases.

21 Figure 2 investigates the effect of the size of the damage blocks. Again, results are for a  
22 lattice with 25% dead sites, a linear size  $L = 256$ , stress dissipation  $\alpha = 0$ , and a stress transfer  
23 range of  $R = 16$ . The dead block size,  $b$ , is varied while the interaction length,  $R$ , remains  
24 constant. In this case, the scaling regime and maximum event size increases as the ratio  $R/b$   
25 decreases. The spatial distribution of  $\gamma_i$  affects the potential for a large event because failing

1 sites with low values of  $\gamma_i$  pass along a high percentage of excess stress to neighboring sites,  
2 encouraging additional failures. In the damage only system, site dissipation is determined by  
3 spatial locality only, so we require large clumps of sites with low values of  $\gamma_i$  in order to allow  
4 for a large event.

5 In this work, the focus is also on the spatial heterogeneity in OFC models with long-range  
6 stress transfer. The model is a cellular automata version of earthquake faults based on the  
7 OFC (Olami et al., 1992) and RJB (Rundle and Jackson, 1977; Rundle and Brown, 1991)  
8 models with some minor variations. Here, inhomogeneities are imposed in the model by  
9 allowing a percentage of randomly selected locations that accumulate higher levels of stress,  
10 similar to asperities on natural faults. These sites are incorporated by varying the ability of  
11 individual sites to support much higher stress for different spatial configurations. We find that  
12 the scaling relationship for the heterogeneous systems depends on the amount of the asperity  
13 sites as well as the spatial distribution of those asperities and the ratio of the size of the  
14 asperities to the stress transfer range. Investigation of the effects of a variety of spatial  
15 configurations for asperity sites provides insights into the construction of practical models of  
16 an earthquake fault system which is consistent with GR scaling.

17

## 18 **2 The Model**

19 Our model is a two-dimensional cellular automaton model with periodic boundary conditions.  
20 In this model every site in the lattice is connected to  $z$  neighbors, which are defined as sites  
21 within a certain distance or stress interaction range,  $R$ . A homogeneous residual stress  $\sigma^r$  is  
22 assigned to all the sites in the lattice. To impose spatial inhomogeneity on the lattice, two sets  
23 of failure thresholds are introduced; ‘regular sites’ with a constant failure threshold of  $\sigma^F$  and  
24 ‘asperity sites’ with a much higher failure threshold ( $\sigma^F_{(asperity)} = \sigma^F + \Delta\sigma^F$ ). These asperity sites

1 are imposed in order to incorporate some percentage of stronger sites into the lattice which  
2 will bear higher stress before failure.

3 Initially, the internal stress variable,  $\sigma_i(t)$ , is randomly distributed on each site in such a way  
4 that the stress on all sites lies between the residual and failure stress thresholds  
5 ( $\sigma^r < \sigma_i(t=0) < \sigma^F$ ). At  $t=0$  no sites will have  $\sigma_i > \sigma^F$ . There are several ways to simulate the  
6 increase in stress associated with the dynamics of plate tectonics. Here we use the so-called  
7 zero velocity limit (Olami et al., 1992). The entire lattice is searched for the site that  
8 minimizes  $(\sigma^F - \sigma_i)$  and that amount of stress is added to each site such that the stress on at  
9 least one site is now equal to its failure threshold. That site fails and some fraction of its  
10 stress, given by  $\alpha [\sigma^F - (\sigma^r \pm \eta)]$ , is dissipated from the system.  $\alpha$  is a dissipation parameter  
11 ( $0 < \alpha \leq 1$ ) which describes the portion of stress dissipated from the failed site and  $\eta$  is randomly  
12 distributed noise. The failed site's stress is lowered to  $(\sigma^r \pm \eta)$  and the remaining stress is  
13 distributed to its neighbors. After the first site failure, all neighbors are searched to determine  
14 if the stress change from the failed site caused any of others to reach their failure stress. If so,  
15 the described procedure repeats for those neighbors and if not, the time step (known as the  
16 plate update) increases by unity and the lattice is searched again for the next site which  
17 minimizes  $(\sigma^F - \sigma_i)$ . The size of the event is calculated from the total number of failures that  
18 expand from the first failed site. Stress is dissipated from the system both at the regular lattice  
19 sites and through asperity sites which are placed inhomogeneously throughout the lattice.  
20 However, because the asperity sites release much higher stress at the time of their failure, the  
21 amount of stress dissipated by these sites is different from the bulk of the system and results  
22 in inhomogeneous stress dissipation in this model.

23 Initial results for two different sized large asperity blocks are shown in Figure 3 (a-5% and b-  
24 10% of the total lattice sites are considered as asperity sites), with their associated magnitude-

1 frequency relation plotted for varying values of  $\alpha$ . Both plots support previous results that  
2 increasing values of stress dissipation decrease the length of the scaling regime and the time  
3 of the largest events, and that larger asperity, or damage, regions promote the occurrence of  
4 larger events.

5 In this study we want to investigate the scaling in these systems for different percentages of  
6 asperity sites and different asperity configurations, comparing those results with the simple  
7 homogeneous system with no asperities.

8

### 9 **3 Percentage of asperity blocks**

10 A system with different percentage of randomly distributed asperity sites in a two  
11 dimensional cellular automaton lattice of linear size  $L=256$  with periodic boundary conditions  
12 and long range of interaction ( $R=16$ ) is studied here. In this model we consider a  
13 homogeneous failure threshold for the regular sites of  $\sigma^F=2.0$ , a homogeneous residual stress  
14 for the entire lattice of  $\sigma^r=1.0$ , and a random distribution of noise as  $\eta=[-0.1,+0.1]$ . The failure  
15 threshold for the asperity sites is  $\sigma^F_{(asperity)}=\sigma^F+10$ . Figure 4 shows the distribution of event  
16 sizes for different cases where  $\alpha$  is equal to 0.2. This study begins with smaller percentages of  
17 asperities and increase the number of randomly distributed stronger sites in the lattice (no  
18 asperities in black, 1% in blue, 3% in green and 5% in red). As the percentage of asperities  
19 increases, the system produces significantly larger events. However, the relative number of  
20 moderate-sized events decreases as the number of asperities in the lattice is increased. By  
21 increasing the number of asperities in the lattice some of the moderate events appear to grow  
22 into a larger event. This migration from the moderate to large sizes could be consequence of  
23 two effects. When an asperity site breaks a greater amount of stress is released into the system  
24 and that amount of released stress can cause the failure of more sites and result in larger

1 events, especially in a system with long range stress transfer. In addition, a greater number of  
2 randomly distributed asperity sites in the lattice increases the probability of asperity sites  
3 triggering. In other words, a system with a higher density of asperities increases the chance of  
4 asperity blocks to be in the stress transfer range of another asperity. So, failure of one asperity  
5 site can results in a cascade behavior and a greater likelihood for a medium size event to grow  
6 and become an extreme event.

7

#### 8 **4 Configuration of spatial heterogeneity**

9 Dominguez et al. (2013) studied the scaling behavior of systems with damage and showed  
10 that event distribution depends not only on the total amount of damaged sites in the system  
11 but also on the spatial distribution of damage. They noticed that lattices with more  
12 homogeneously distributed dead sites suppress large events. Here, we study the effect of  
13 different spatial configurations of the asperity blocks in the system. In this model, the lattices  
14 have the same size ( $256 \times 256$ ), a constant percentage of asperity sites (1% and 5% for each  
15 case), and a constant stress transfer range ( $R = 16$ ). As a result, any differences in the large  
16 event behavior are not caused by the finite size of the lattice. Figure 5 presents two-  
17 dimensional lattices of linear size  $L = 256$  and asperity blocks with a linear size of  $b$  which  
18 are randomly distributed throughout the system and two cases of 1% (top) and 5% (bottom) of  
19 asperity sites (note that the stress dissipation parameter is constant in all cases,  $\alpha = 0.2$ ). To  
20 highlight the distinction between the different configurations of asperities, logarithmic bins  
21 are used in the distributions and they are normalized to the total number of events in each  
22 case. Figure 6 shows the probability density function of event sizes for the various  
23 arrangements of asperity blocks in Figure 5. By changing the linear size of the asperity  
24 blocks, we ensure that at least some of the asperity sites which are inside a larger asperity

1 block are in the stress transfer range of others and will certainly interact with each other. On  
2 the other hand, we decrease the probability of interaction between two large blocks of asperity  
3 sites. Although the number of asperity sites is constant, changing the linear size of the  
4 asperity sites has a significant effect on the event distributions. For 1% of asperities,  $b=1$   
5 (Figure 5a-i) has the lowest spatial separation among the different size of asperity blocks. But  
6 since there are fewer of asperities in the lattice, the probability of interaction between the  
7 asperity sites is still very low and big events do not occur even with the failure of an asperity  
8 site. For  $b=4$ , there are 16 asperity sites in a 4 by 4 block that are adjacent to each other.  
9 Failing a site in the asperity block can easily trigger the rest of the block and create larger  
10 events than for  $b=1$  (Figure 6a). The numerical distributions for  $b=8$  and  $b=16$  confirms that  
11 there is triggering of asperity sites inside the block, but because the distance between the  
12 blocks is higher than the stress transfer range they cannot affect each other directly. Again, in  
13 this case the largest events occur for smaller values of  $R/b$ .

14 The biggest event for 5% of asperity sites falls between different configurations of asperity  
15 blocks and occurs for the smallest block size (Figure 6b,  $b=1$ ). Because the percentage of  
16 asperities is much higher, the shortest spatial separation between the asperities occurs in the  
17 case of  $b=1$  and there is a higher probability of asperity triggering. In this case, the number of  
18 triggered asperity sites increases and a much bigger event occurs. However, increasing the  
19 linear size of asperity blocks ( $b=4, 8$  and  $16$ ) increases the probability of triggering inside a  
20 block, but it also increases the spatial separation between the blocks, resulting in a decrease in  
21 the probability of triggering between asperity blocks.

22

## 1    **5    Range of interaction**

2    To further investigate the effect of block size and asperity triggering on event size for larger  
3    numbers of asperities, we focus on the stress transfer range. Here, 5% of asperity sites are  
4    randomly distributed in the system in the blocks with four different linear sizes ( $b=1, 4, 8$  and  
5    16, Figure 5a-ii, b-ii, c-ii and d-ii) and the system is run for three different stress transfer  
6    ranges,  $R=16$ ,  $R=8$  and  $R=1$ . Figure 7 shows the comparison between the event distributions  
7    for different stress transfer ranges and different asperity block sizes. By reducing the stress  
8    transfer range, the likelihood that an asperity site will be affected by a neighboring asperity  
9    site decreases. This results in a lower probability of asperity triggering in the model. The  
10    absence of triggering asperities makes the system unable to produce big events. Figure 7  
11    confirms that, for lower percentages of asperities, the size of the biggest event occurs in  
12    systems with long range interactions ( $R=16$ ), regardless of the asperity block size, and that  
13    event is much larger than the size of the biggest event in system with short stress transfer  
14    range. In addition, for short range stress transfer ( $R=1$ ), the size of the largest events does not  
15    change with increasing asperity block size. For longer range stress transfer, the size of the  
16    asperity blocks affects the size of the biggest event.

17

## 18    **6    Stress dissipation**

19    We also compare the effect of stress dissipation parameters on different asperity  
20    configurations in a system with long stress transfer range,  $R=16$ . As discussed earlier, upon  
21    failure, some fraction of a site's stress, given by  $\alpha [\sigma^F - (\sigma' \pm \eta)]$ , is dissipated from the system  
22    ( $0 < \alpha \leq 1$ ). In general, lower stress dissipation models produce more larger events and higher  
23    stress dissipation suppresses large events. This also should be true in the system with asperity  
24    sites. In higher dissipation models, less stress is transferred to neighboring sites, even when

1 asperities fail. As a result, there is lower probability of asperity triggering in the model. This  
2 implies smaller events and more plate update steps to fail all of the asperities. In Figure 8 the  
3 event distribution for four different stress dissipation parameters and 1% of asperity sites in  
4 the lattice is compared for three different configuration of asperity blocks ( $b=1$ ,  $b=4$  and  
5  $b=16$ ). This figure shows the results for four stress dissipation parameters,  $\alpha=0.2, 0.3, 0.4$  and  
6  $0.5$ , in each 20%, 30%, 40% and 50% of the failed site stress dissipates at the time of failure  
7 and the remaining stress is distributed to its  $z=1088$  neighbors. For all three asperity  
8 configurations (Figure 8 a, b and c), lower values of stress dissipation leads to a higher  
9 number of big events. On the other hand, in systems with a high amount of stress dissipation,  
10 the released stress from a small asperity block is not enough to offset the greater dissipation  
11 and cannot trigger any of the neighboring asperity blocks. As a result, the change in the  
12 asperity block size from  $b=1$  to  $b=4$  (Figure 8a and 8b) does not significantly affect the  
13 distributions of events, especially for higher stress dissipation. However, the released stress  
14 from bigger asperity blocks of  $b=16$  is high enough to trigger another asperity block. We  
15 again observe larger events in the tail of the distributions, even for higher stress dissipation  
16 models (Figure 8c).

17

## 18 **7 Conclusions**

19 Here we investigated a variation of the OFC model in which localized stress accumulators  
20 were added to the system by converting a small percentage of the lattice site into stronger  
21 sites. We studied different spatial configurations of the stronger asperity sites and observed  
22 the effect of asperity patterns on the distribution of event sizes in the systems for a selected  
23 stress transfer range. In particular, we observed an increasing number of larger events  
24 associated with the total number of asperities in the lattice (Figure 4). We also found that

1 imposing a fixed number of asperity sites with different spatial distributions strongly affects  
2 the capability of the fault system to generate extreme events, but that the total percentage of  
3 asperities is important as well. The event distributions shown in Figure 6 confirm the  
4 sensitivity of the system to different configurations of inhomogeneities. In addition, we  
5 studied the role of the interaction range on triggering asperities and observed that the  
6 probability of asperity triggering and the occurrence of larger events is much higher in the in  
7 those systems with a longer stress transfer range (Figure 7). However, in models with higher  
8 dissipation it is the asperities are less sensitive to other failures and therefore the probability  
9 of asperity triggering decreases in high dissipation models. This implies that higher  
10 dissipation results in a lower probability of smaller events regardless of the number and  
11 spatial distribution of asperities.

12

### 13 **Acknowledgements**

14 This research was funded by the NSERC and Aon Benfield/ICLR IRC in Earthquake Hazard  
15 Assessment, and an NSERC Discovery Grant (JK and KFT).

16

17

18

19

20

21

22

## 1 **References**

- 2 Alava, M. J., Nukala, P., and Zapperi, S. (2006), Statistical models of fracture, *Adv. Phys.* 55,  
3 349.
- 4 Bach, M., Wissel F. and Dressel, B. (2008), Olami-Feder-Christensen model with quenched  
5 disorder. *Phys. Rev. E* 77, 067101.
- 6 Burridge, R., Knopoff, L. (1967), Model and theoretical seismicity, *Bull. Seismol. Soc. Am.*  
7 57. 341–371.
- 8 Carlson, J. M. and Langer, J. S. (1989), Mechanical model of an earthquake fault. *Phys. Rev.*  
9 *Lett.* 62, 2632; *Phys. Rev. A* 40, 6470.
- 10 Ceva, H. (1995), Influence of defects in a coupled map lattice modelling earthquakes. *Phys.*  
11 *Rev.* E52, 154.
- 12 Dahmen, K., Ertas, D., and Ben-Zion, R. (1998), Gutenberg-Richter and Characteristic  
13 Earthquake Behavior in Simple Mean-field Models of Heterogeneous Faults, *Phys. Rev. E* 58,  
14 1494–1501.
- 15 Dominguez, R., Tiampo, K.F., Serino, C.A. and Klein W. (2013), Scaling of earthquake  
16 models with inhomogeneous stress dissipation. *Phys. Rev. E* 87, 022809.
- 17 Gutenberg, B. and Richter, C.F. (1956), Magnitude and energy of earthquakes. *Annali di*  
18 *Geofisica*, Vol. 9, n. 1.
- 19 Herz, A.V.M., and Hopfield, J.J. (1995), Earthquake Cycles and Neural Reverberations,  
20 Collective Oscillations in Systems with Pulse-Coupled Threshold Elements. *Phys. Rev. Lett.*,  
21 75, 1222-1225.
- 22 Jagla, E.A. (2010), Realistic spatial and temporal earthquake distributions in a modified  
23 Olami-Feder-Christensen model. *Phys. Rev.* E81, 046117.

- 1 Janosi, I.M. and Kertesz, J. (1994), Self-organized criticality with and without conservation.  
2 *Physica A*200, 0378.
- 3 Kanamori, H. (1981), The nature of seismicity patterns before large earthquakes, in  
4 *Earthquake Prediction, Maurice Ewing Series, IV*, 1–19, AGU, Washington D.C..
- 5 Klein, W., Gould, H., Gulbahce, N., Rundle, J. B. and Tiampo, K. (2007), Structure of  
6 fluctuations near mean-field critical points and spinodals and its implication for physical  
7 processes. *Phys. Rev. E* 75, 031114.
- 8 Lyakhovsky, V. and Ben-Zion, Y. (2009), Evolving geometrical and material properties of  
9 fault zones in a damage rheology model, *Geochem. Geophys. Geosyst.*, 10, Q11011.
- 10 Main, I. (1996), Statistical physics, seismogenesis, and seismic hazard. *Rev. Geophys.* 34,  
11 433–462.
- 12 Mousseau, N. (1996), Synchronization by Disorder in Coupled Systems. *Phys. Rev. Lett.* 77,  
13 968.
- 14 Nakanishi, H. (1990), Cellular-automaton model of earthquakes with deterministic dynamics.  
15 *Phys. Rev. A* 41, 7086.
- 16 Olami, Z., Feder, HJS., Christensen, K. (1992), Self-organized criticality in a continuous,  
17 nonconservative cellular automaton modelling earthquakes. *Phys Rev Lett* 68(8):1244–1247.
- 18 Ogata, Y. (1983), Estimation of the parameters in the modified Omori formula for aftershock  
19 frequencies by the maximum likelihood procedure, *Journal of Physics of the Earth*, Vol.31,  
20 115-124.
- 21 Otsuka, M. (1972), *Phys Earth Planet Inter.* 6-311.
- 22 Ramos, O., Altshuler, E. and Maloy K.J. (2006), Quasiperiodic Events in an Earthquake  
23 Model. *Phys. Rev. Lett.* 96, 098501.

1 Rundle, J.B., Turcotte, D.L., Shcherbakov, R., Klein, W., Sammis, C.,(2003), Statistical  
2 physics approach to understanding the multiscale dynamics of earthquake fault systems.  
3 *Review of Geophysics*, 41, 1019.

4 Rundle, J. B., Klein, W., Tiampo, K. and Gross S., (2000), Linear pattern dynamics in  
5 nonlinear threshold systems, *Phys. Rev. E*, 61 (3), 2418–2431.

6 Rundle, JB, Klein W. and Gross S. (1999), Physical basis for statistical patterns in complex  
7 earthquake populations: Models, predictions, and tests, *PAGEOPH*, 155, 575-607.

8 Rundle, J. B. and Brown, S. R. (1991), Origin of Rate Dependence in Frictional Sliding, *J.*  
9 *Stat. Phys.* 65, 403.

10 Rundle, J. B. (1988), A physical model for earthquakes, *J. Geophys. Res.* 93-6237.

11 Rundle, J. B. and Jackson, D. D. (1997), Numerical simulation of earthquake sequences, *Bull.*  
12 *Seismol. Soc. Am.* 67.

13 Serino, C. A., Tiampo, K. F. and Klein W. (2011), New Approach to Gutenberg-Richter  
14 Scaling, *Phys. Rev. Lett.* 106, 108501.

15 Scholz, C.H. (2002), *The mechanics of earthquakes and faulting*, Cambridge University Press,  
16 p. 471.

17 Schorlemmer, D., and Gerstenberger, M. C. (2007), RELM testing center, *Seismol. Res. Lett.*  
18 78, 1, 30-36.

19 Tiampo, K. F., Rundle, J. B., Klein, W., Holliday, J., S´aMartins, J. S. and Ferguson, C. D.  
20 (2007), Ergodicity in natural earthquake fault networks. *Phys. Rev. E* 75, 066107.

21 Tiampo, K.F., Rundle, J.B., McGinnis, S., Gross, S., Klein, W. (2002), Mean-field threshold  
22 systems and phase dynamics: an application to earthquake fault systems. *Eur. Phys. Lett.* 60,  
23 481–487.

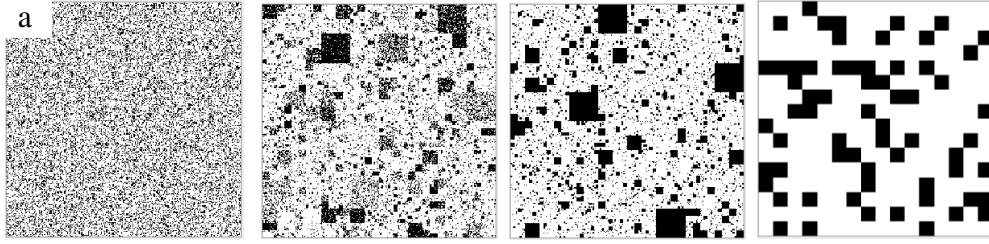
- 1 Torvund F., and Froyland, J. (1995), Strong ordering by non-uniformity of thresholds in a  
2 coupled map lattice. *Physica Scripta* 52, 624.
- 3 Turcotte, D.L., Newman, W.I., Shcherbakov, R. (2003), Micro and macroscopic models of  
4 rock fracture. *Geophysical Journal International* 152, 718–728.
- 5 Turcotte, D. L. (1997), *Fractals and chaos in geology and geophysics*, 2nd edn. Cambridge,  
6 UK: Cambridge University Press.
- 7 Utsu, T., Ogata, Y. and Matsu'ura, R. S. (1995), The centenary of the Omori formula for a  
8 decay law of aftershock activity, *Journal of Physics of the Earth*, Vol.43, pp.1-33.
- 9 Vere-Jones, D. (2006), The development of statistical seismology, A personal experience.  
10 *Tectonophysics* 413, 5–12.
- 11 Vere-Jones, D. (1995), Forecasting earthquakes and earthquake risk. *International Journal of*  
12 *Forecasting* 11, 503–538.
- 13 Zechar, J.D., Jordan, T.H. (2010), Simple smoothed seismicity earthquake forecasts for Italy.  
14 *Annals of Geophysics* 53.

1

2

3

4



5

6

7

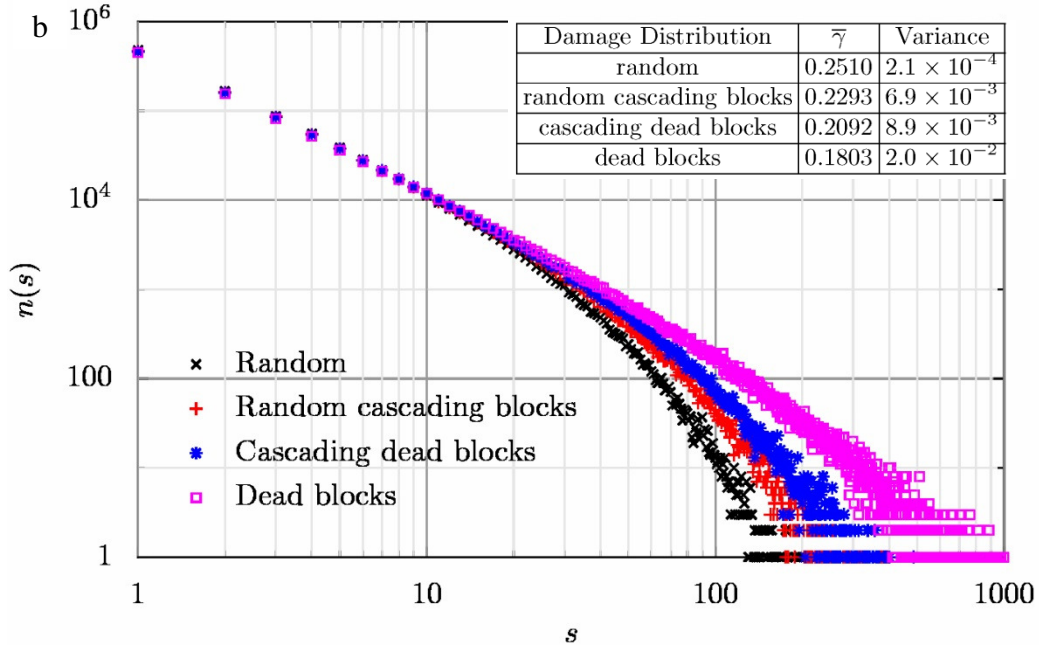
8

9

10

11

12



13 Figure 1. a) Various configurations of 25% dead sites (in black) for a lattice with  $\alpha = 0$  and a

14 linear size  $L = 256$ . From left to right, lattices contain dead sites distributed randomly

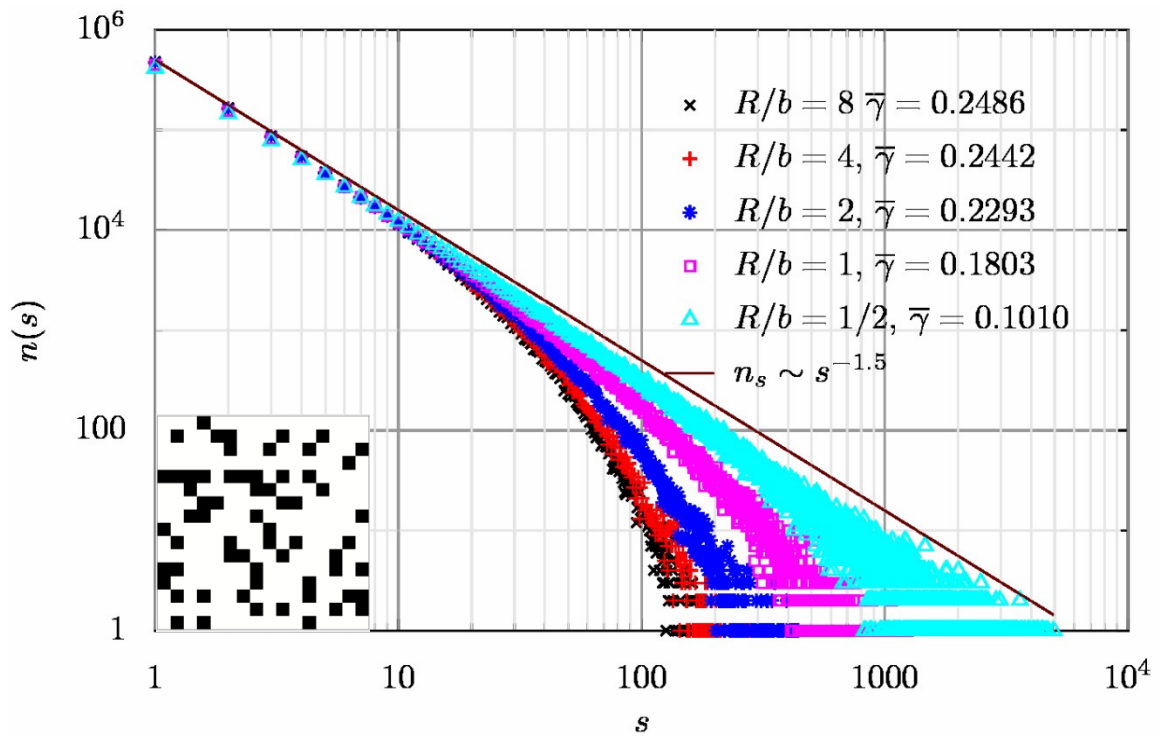
15 (random), blocks of various sizes, where each block has varying values of randomly

16 distributed dead sites (random cascading blocks), completely dead blocks of various sizes

17 (cascading dead blocks), and dead blocks of a uniform size (dead blocks); b) Numerical

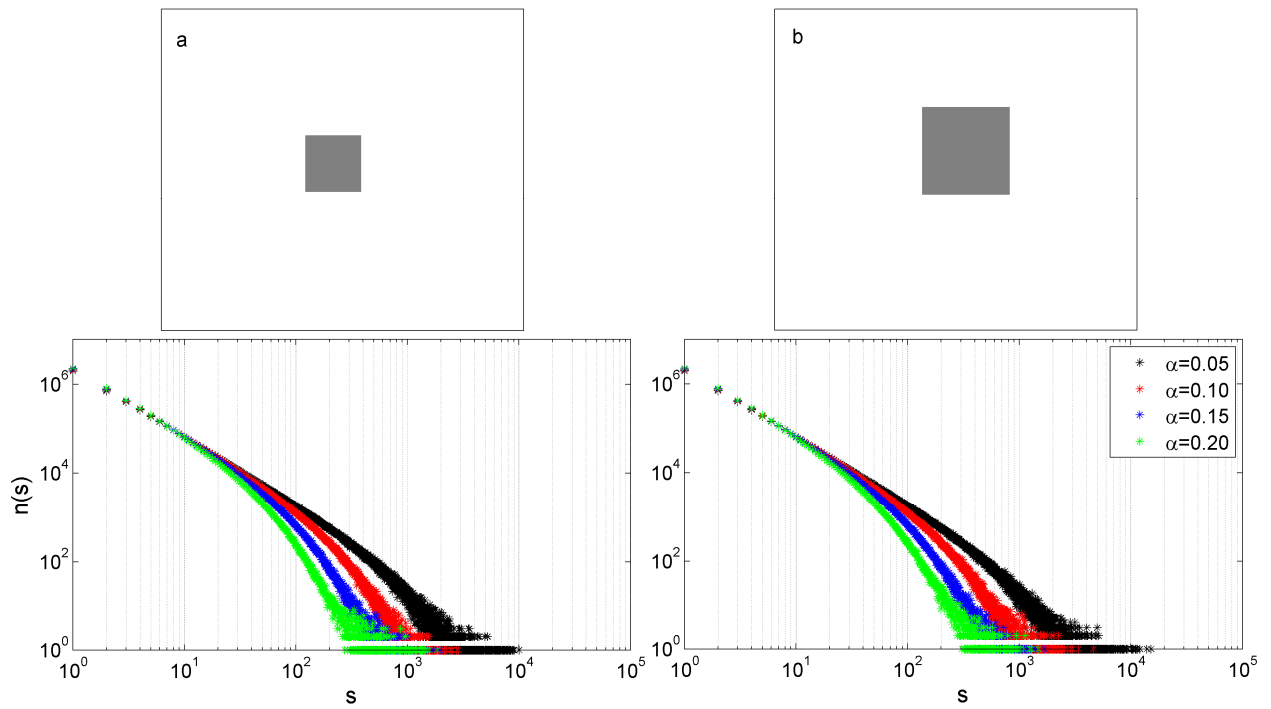
18 distribution of avalanche events of size  $s$  for the various spatial distributions of dead sites

19 shown in (a) with stress transfer range  $R = 16$ .  $\bar{\gamma}$  is the average dissipation for each lattice.



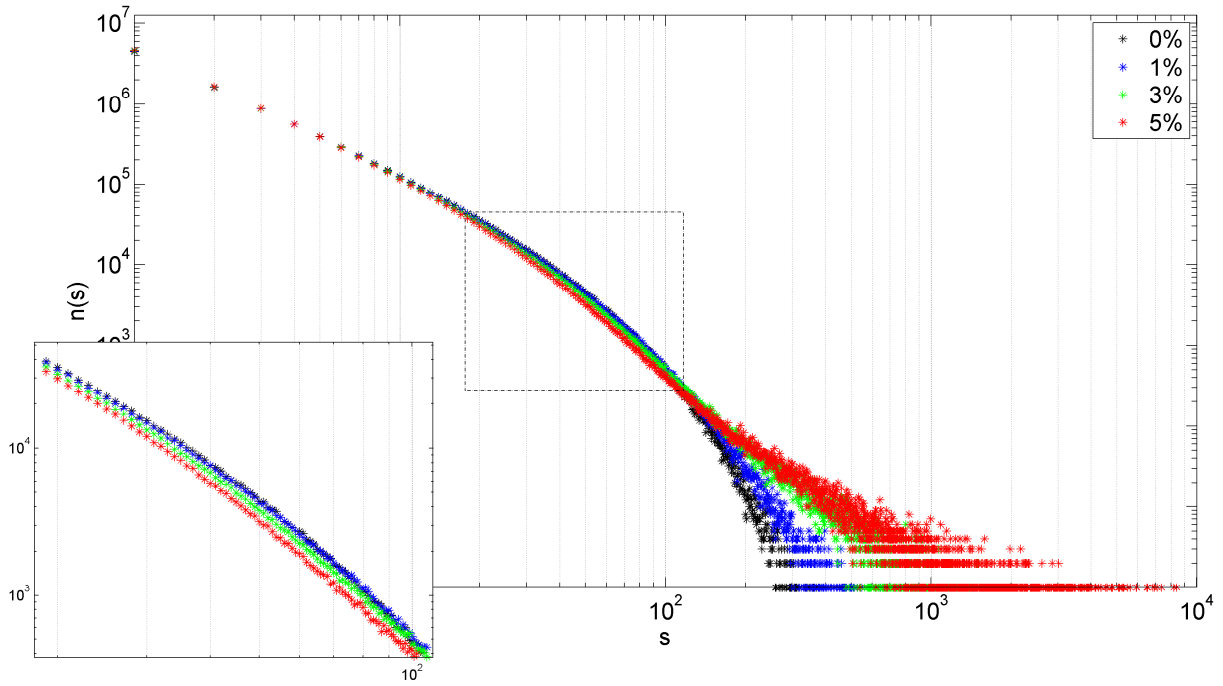
1 Figure 2. Numerical distribution of avalanche events of size  $s$  for blocks of dead sites of  
 2 linear size  $b$ . Systems are characterized by the dimensionless parameter  $R/b$ . (the inset  
 3 corresponds to  $R/b = 1$ .) The size of the systems shown here is  $L = 256$ ,  $\alpha = 0$ , and the stress  
 4 transfer range is  $R = 16$ .

5  
 6  
 7  
 8  
 9  
 10  
 11  
 12



1  
 2 Figure 3. a) Schematic depicting the size and location of a smaller set (5% of the total lattice  
 3 sites) of grouped asperities (top). Numerical distribution of event sizes for varying values of  
 4 stress dissipation,  $\alpha$ , for the layout shown above. b) Schematic depicting the size and location  
 5 of the larger set (10% of the total lattice sites) of grouped asperities (top). Numerical  
 6 distribution of event sizes for varying values of stress dissipation,  $\alpha$ , for the layout shown  
 7 above.

8



1

2 Figure 4. Numerical distribution of events of size “s” for various amounts of randomly  
 3 distributed asperity sites,  $\alpha=0.2$ .

4

5

6

7

8

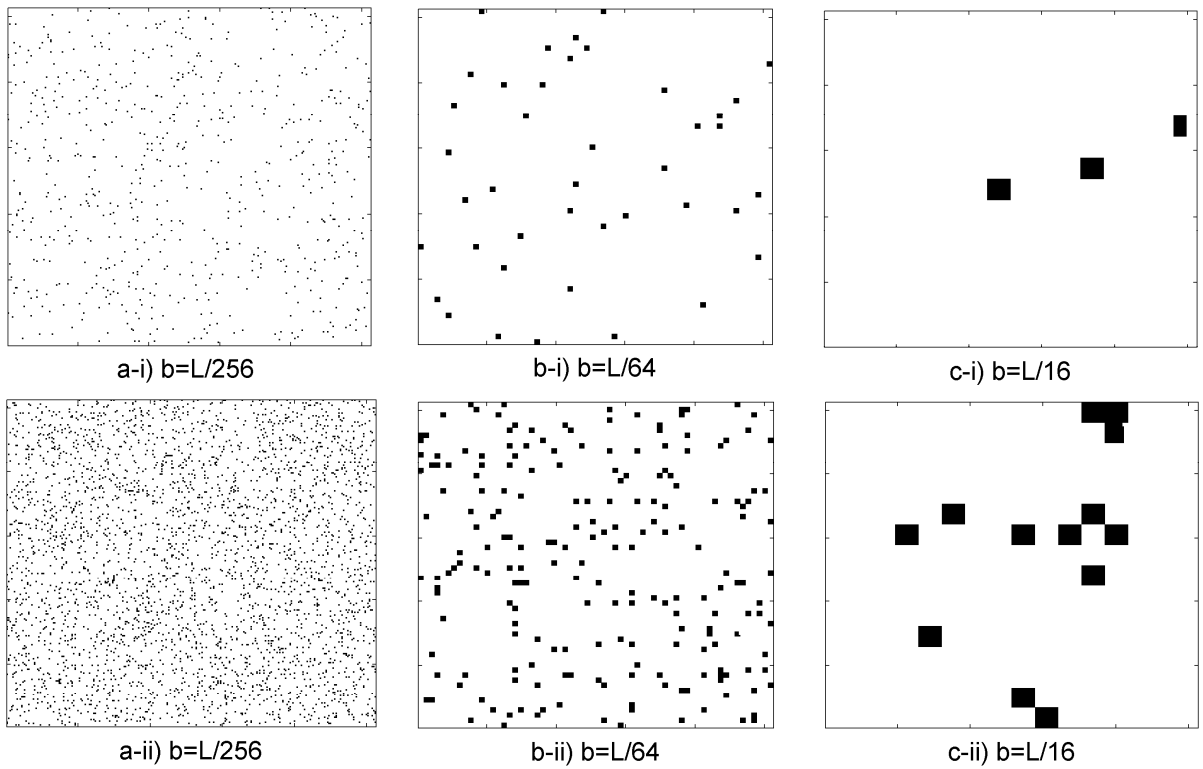
9

10

11

12

13



1

2 Figure 5. Four different configurations of 1 percent asperity sites (upper row) and 5 percent  
 3 asperity sites (lower row) (in black) for lattices with linear size  $L=256$ . Each lattice has  
 4 asperity blocks of a single size  $b$ . For each **a)**  $b=L/256$ , **b)**  $b=L/64$ , **c)**  $b=L/32$ , and **d)**  $b=L/16$ .

5

6

7

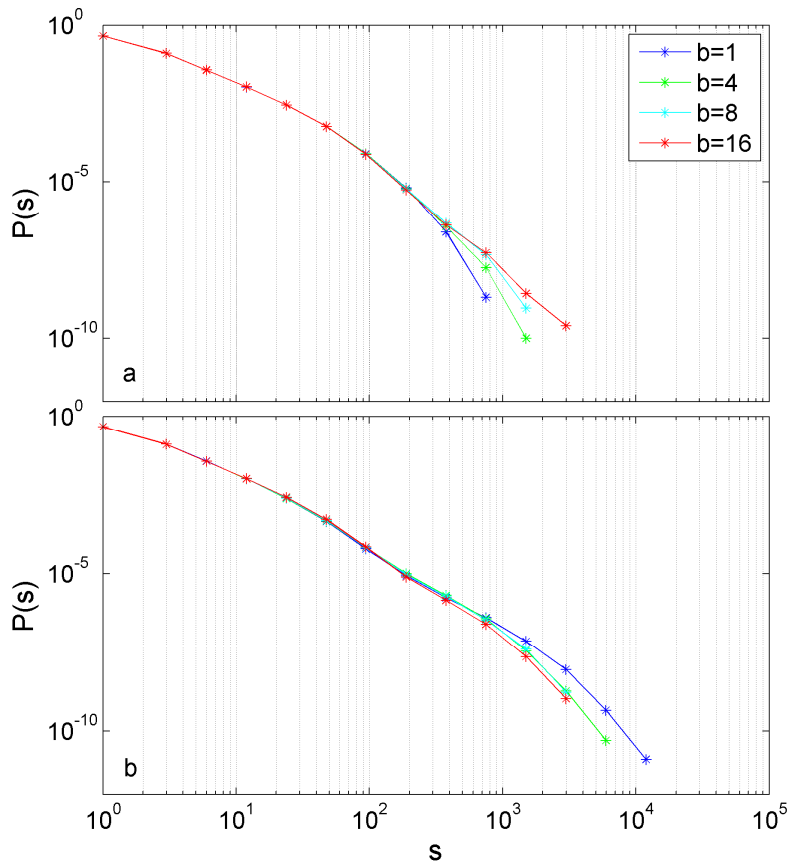
8

9

10

11

12



1

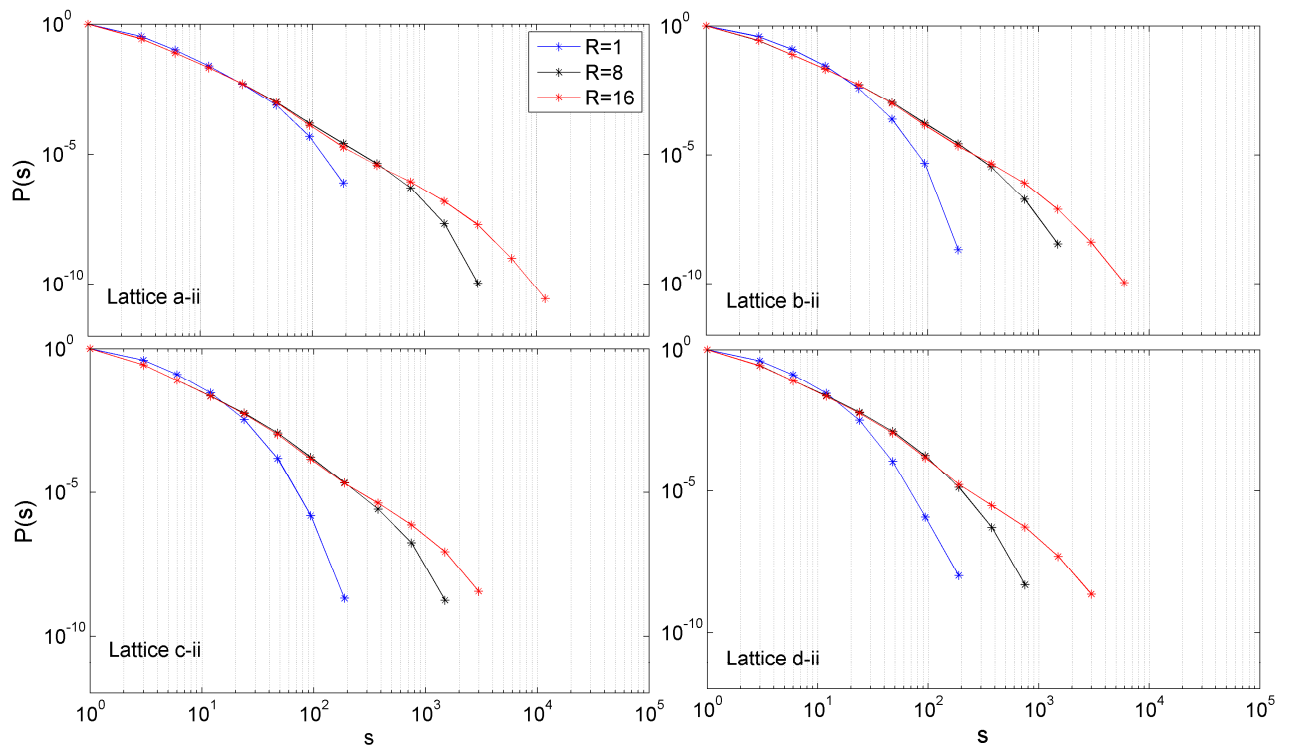
2 Figure 6. Normalized probability density function of events of size “s” for various sizes of  
 3 asperity blocks which are randomly distributed in the system for  $R=16$  and **a)** 1% and **b)** 5%  
 4 of asperity sites.

5

6

7

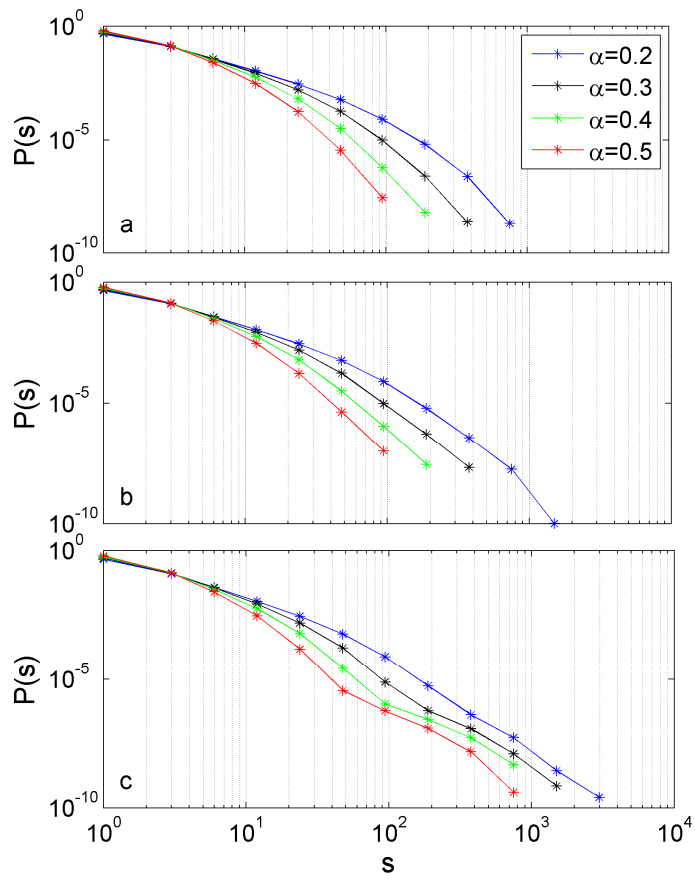
8



1

2 Figure 7. Normalized probability density function of events of size  $s$  for various stress transfer  
 3 range in a system with 5% of asperity sites for four different linear sizes of asperity blocks  
 4 shown in Figure 2 and **a)**  $b=1$ , **b)**  $b=4$ , **c)**  $b=8$  and **d)**  $b=16$ .

5



1

2 Figure 8. Normalized probability density function of events of size  $s$  for various amount of  
 3 stress dissipation parameter and for 1% of three different sizes of asperity blocks randomly  
 4 distributed in the system for **a)**  $b=1$ , **b)**  $b=4$  and **c)**  $b=16$ .